

Control of the Color Contrast of a Polychromatic Light-Emitting Device With CdSe–ZnS Nano-Crystals on an InGaN–GaN Quantum-Well Structure

Dong-Ming Yeh, Chi-Feng Huang, Horng-Shyang Chen, Tsung-Yi Tang, Chih-Feng Lu, Yen-Cheng Lu, Jian-Jang Huang, C. C. Yang, I-Shuo Liu, and Wei-Fang Su

Abstract—Blue-red polychromatic light-emitting devices are fabricated by attaching red-emitting CdSe–ZnS nano-crystals on a blue-emitting InGaN–GaN multiple-quantum-well (MQW) structure. To improve the red/blue intensity contrast, holes of different diameters are fabricated for increasing the direct contact area between the MQW active regions and CdSe–ZnS nano-crystals. By comparing the devices of 10-, 50-, 60-, and 70- μm hole diameters, and a reference device of no hole, it is found that the hole diameter of 60 μm represents an optimized condition from the viewpoint of maintaining high quantum efficiency. However, the device of 10- μm holes has the highest red/blue intensity ratio, which corresponds to a 36% increase. This result is attributed to its largest side-wall area in the holes among various samples.

Index Terms—CdSe–ZnS nano-crystal, InGaN–GaN quantum well, light-emitting device, white light.

IN developing white-light source for energy-saving solid-state lighting and liquid-crystal-display back-lighting, the GaN-based light-emitting diode (LED) has been an issue of much attraction. Currently, several techniques are used for LED white-light generation. First, three different phosphors are attached on an ultraviolet (UV) LED to transfer the emitted UV photons into blue, green, and red lights for white-light generation [1]. Second, green and red phosphors are coated on an InGaN-based blue-emitting LED for producing white light [2]. Third, yellow phosphor is placed on a blue LED for mixing blue and yellow lights to become white [3], [4]. Fourth, three LEDs of the three elemental colors based on different semiconductors are closely arranged for white-light mixing [5]. However, to improve the quantum efficiency and reduce the fabrication cost, the single-chip all-semiconductor white-light LED has been a target of research effort. Nevertheless, although the fabrications of highly efficient blue and green nitride-based

LEDs have been quite mature, that of the yellow or red LED requires much more effort. Recently, InGaN-based red LEDs have been reported [6], [7]. However, for such a device, either the quantum efficiency needs to be improved or the process technique needs to be developed.

Recently, an alternative approach for red light generation was proposed [8]. In this approach, CdSe–ZnS nano-crystals are coated on a nitride-based multiple-quantum-well (MQW) structure for receiving electron–hole pairs excited in the MQW region. Such a nano-crystal consists of a CdSe core of a few nanometers in diameter and a ZnS shell of a few tenths nanometers in thickness [9]. It acts as a quantum dot for receiving electron–hole pairs and emitting long-wavelength photons. Such a Forster transfer process can be used for efficiently generating multicolor light from a short-wavelength-emitting LED. However, for an efficient Forster-transfer process, the MQW structure must be very close to the nano-crystals. Hence, the fabrication of such a practical device becomes complicated. Another process in such a device structure for multicolor generation includes the absorption of short-wavelength photons and then the reemission of the long-wavelength light through the nano-crystals. The absorption and emission wavelengths of the nano-crystals can be easily adjusted by changing their core sizes [10], [11]. Therefore, nano-crystals with strong absorption in the UV-blue range and efficient emission in the yellow-red range can be obtained.

In a multicolor light-emitting device for white-light generation, the intensity ratios of different colors are important parameters for controlling the color rendering index. Normally, the short-wavelength light, generated directly from semiconductor quantum wells, is stronger than that of energy-transfer generation. Such a contrast can be improved by increasing the carrier transfer into the nano-crystals or the absorption efficiency of the nano-crystals through the increase of the contact area between the nano-crystals and the MQW active regions. In this letter, we report the control of color contrast in a two-color light-emitting device with red-emitting CdSe–ZnS nano-crystals on a blue-emitting InGaN–GaN MQW LED by etching holes on top of the LED surface. The holes were etched deep down to the active layers and filled up with the CdSe–ZnS nano-crystals such that the nano-crystals can directly contact the MQW regions. The direct contact implies more efficient

Manuscript received October 24, 2005; revised December 8, 2005. This work was supported by the National Science Council, The Republic of China, under Grant NSC 93-2210-M-002-006 and Grant NSC 94-2215-E-002-015, and by the U.S. Air Force under Contract AOARD-04-4026 and Contract AOARD-05-4085.

D.-M. Yeh, C.-F. Huang, H.-S. Chen, T.-Y. Tang, C.-F. Lu, Y.-C. Lu, J.-J. Huang, and C. C. Yang are with the Graduate Institute of Electro-Optical Engineering and Department of Electrical Engineering, National Taiwan University, Taipei 10617, Taiwan, R.O.C. (e-mail: ccy@cc.ee.ntu.edu.tw).

I.-S. Liu and W.-F. Su are with the Department of Material Science and Engineering, National Taiwan University, Taipei, Taiwan 10617, R.O.C.

Digital Object Identifier 10.1109/LPT.2006.870056

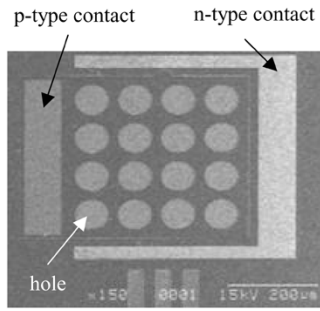


Fig. 1. SEM image of etched holes of $70\ \mu\text{m}$ in diameter on the top of a blue LED for filling up with CdSe–ZnS nano-crystal solution.

Forster transfer and absorption-reemission processes. With such a structure, the red/blue contrast ratio can be enhanced even though the total intensity is slightly sacrificed.

The blue-emitting MQW structure was grown on (0001) sapphire substrate with metal–organic chemical vapor deposition and consists of a 25-nm GaN buffer layer, a $2\text{-}\mu\text{m}$ Si-doped GaN, five periods of 3 nm/18 nm InGaN–GaN MQW layers, and an 80-nm Mg-doped GaN epilayer. The emission wavelength is about 450 nm. Circular holes of various diameters were fabricated with the techniques of photolithography and inductively coupled plasma reactive ion etching. The etching depth was $1.2\ \mu\text{m}$. In other words, the active MQW layers were removed in the hole areas. For comparison, samples of hole diameters at 10, 50, 60, and $70\ \mu\text{m}$ were prepared. Fig. 1 shows the scanning electron microscopy (SEM) image on the top surface of the sample with $70\text{-}\mu\text{m}$ holes. A 4×4 hole array on a square area of $400 \times 400\ \mu\text{m}^2$ was fabricated in each sample of 50, 60, or $70\ \mu\text{m}$ in hole diameter. A 15×15 hole array was implemented on the same square area in the sample of $10\ \mu\text{m}$ in hole diameter.

The holes were filled up with toluene solution of CdSe–ZnS nano-crystals. In this process, a droplet of the nano-crystal solution of the same volume was placed on the top of each device. Therefore, the total nano-crystal number in each device is expected to be about the same. By gently shaking the devices, the solution filled up the holes evenly. A uniform layer of nano-crystal still existed on the top surface of each device. The diameter of the CdSe particle is about 4 nm and the thickness of the ZnS shell is about 0.2 nm. The photoluminescence excitation (PLE) spectrum and the photoluminescence (PL) spectrum of the nano-crystal are shown in Fig. 2. The PL detection wavelength in the PLE measurement was set at the PL peak, i.e., 590 nm. An absorption shoulder can be observed in the PLE spectrum, which corresponds to the emission peak of the MQW structure. The blue photons at 450 nm emitted from the MQW structure can be absorbed by the nano-crystals for transferring into red light at 590 nm. Also, carrier transport along a quantum-well layer can transfer electron–hole pairs into nano-crystals in the Forster transfer process.

The current–voltage measurement showed that the device resistance was not significantly changed in fabricating holes of various sizes. The turn-on voltage of all samples, including a reference device of no holes, is around 2.5 V. Fig. 3 shows the electroluminescence (EL) spectra of the samples when the injection current is fixed at 20 mA. Both the blue and red features can be

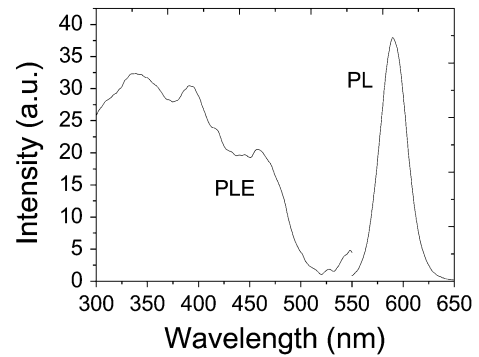


Fig. 2. PLE spectrum detected at 590 nm and PL spectrum of the CdSe–ZnS nano-crystals.

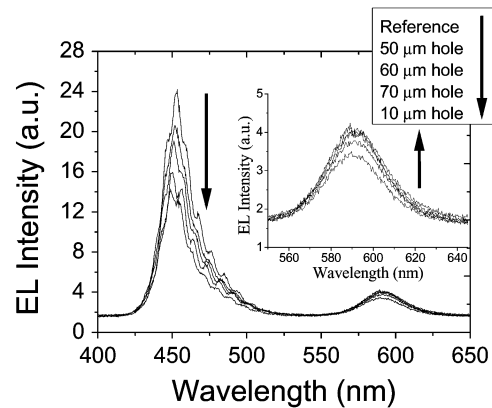


Fig. 3. EL spectra of the fabricated devices with different hole diameters.

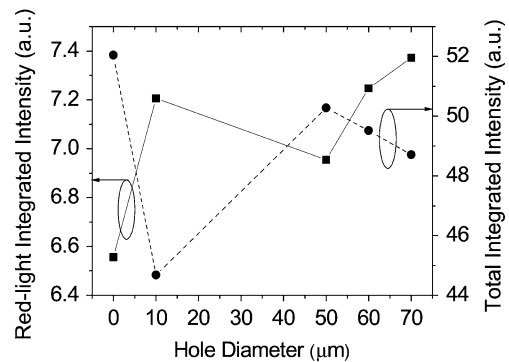


Fig. 4. Variations of the red-light integrated intensity and the total integrated intensity as functions of the hole diameter.

seen. The inset magnifies the spectral portion of red light. One can clearly observe that although red intensity is still weaker than the blue one, the relative intensity of red light is enhanced by fabricating the holes. The vertical arrows show the trends of curve variation following that in the legend. Fig. 4 shows the variations of red-light integrated intensity (the ordinate on the left) and total integrated intensity (the ordinate on the right) as functions of the hole diameter. The data points of zero hole-diameter represent the results of the reference device. One can see that the red-light integrated intensity increases with the hole diameter in the range between 50 and $70\ \mu\text{m}$. However, a smaller hole diameter at $10\ \mu\text{m}$ also results in relatively quite strong red light. This result can be attributed to the larger side-wall area

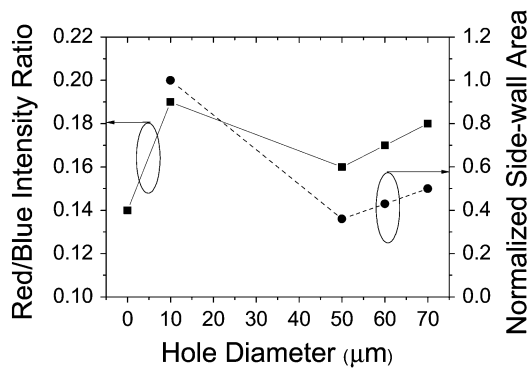


Fig. 5. Variations of the red/blue integrated intensity ratio and the normalized side-wall area as functions of the hole diameter.

in this sample, as to be discussed below (see Fig. 5). The variation trend of the total integrated intensity is opposite to that of the red-light integrated intensity. The reduction of the total integrated intensity is due to the removal of blue-emitting active regions in fabricating the holes. Since the total intensity is still dominated by blue light, the variation of the total integrated intensity is expected to decrease with increasing hole area. The hole area percentages of the samples with 10-, 50-, 60-, and 70- μm holes are 19%, 19%, 28%, and 38%, respectively. This variation trend is consistent with that of the total integrated intensity in the range between 50 and 70 μm . However, the sample of 10- μm holes has quite a low total intensity although only 19% active area was etched. This result can be attributed to the surface state defects on the etched walls, which reduce the internal quantum efficiency of blue emission. Based on the data in Fig. 4, we can calculate the ratios of red intensity increases over blue intensity decreases with respect to the reference device to obtain 0.085, 0.145, 0.155, and 0.112 for the devices of 10-, 50-, 60-, and 70- μm holes, respectively. Therefore, from the viewpoint of maintaining high quantum efficiency, the hole diameter of 60 μm represents an optimized condition.

Fig. 5 shows the variation of the red/blue ratio of the integrated intensity (the ordinate on the left) as a function of the hole diameter. For comparison, the variation of the normalized area of hole side-wall is also shown (the ordinate on the right). In this illustration, the total side-wall area of the 10- μm sample is normalized to unity. One can see that although the red/blue intensity ratio increases with the hole diameter in the range between 50 and 70 μm , the sample of 10- μm holes has the highest ratio, which represents a 36% increase. This variation trend is consistent with that of the normalized side-wall area. The side-wall area is the major factor for producing stronger red intensity and hence a larger red/blue intensity ratio.

In summary, we have fabricated blue-red polychromatic light-emitting devices with red-emitting CdSe-ZnS nano-crystals at-

tached on a blue-emitting InGaN-GaN MQW structure. To improve the red/blue intensity contrast, holes of different diameters were fabricated for increasing the direct contact area between the MQW active regions and CdSe-ZnS nano-crystals. By comparing the devices of 10-, 50-, 60-, and 70- μm hole diameters, and a reference device of no hole, it was found that the hole diameter of 60 μm represented an optimized condition from the viewpoint of maintaining high quantum efficiency. However, the device of 10- μm holes had the highest red/blue intensity ratio, which represented a 36% increase. This result was attributed to its largest side-wall area in the holes among various samples. Because the Forster process is expected to be more efficient in generating the long-wavelength light [8], the limited increase of red-light intensity in our experiment implies that the red-light enhancement is mainly due to the process of absorption and re-emission.

REFERENCES

- [1] J. K. Sheu, S. J. Chang, C. H. Kuo, Y. K. Su, L. W. Wu, Y. C. Lin, W. C. Lai, J. M. Tsai, G. C. Chi, and R. K. Wu, "White-light emission from near UV InGaN-GaN LED chip precoated with blue/green/red phosphors," *IEEE Photon. Technol. Lett.*, vol. 15, no. 1, pp. 18–20, Jan. 2003.
- [2] H. Wu, X. Zhang, C. Guo, J. Xu, M. Wu, and Q. Su, "Three-band white light from InGaN-based blue LED chip precoated with green/red phosphors," *IEEE Photon. Technol. Lett.*, vol. 17, no. 6, pp. 1160–1162, Jun. 2004.
- [3] J. S. Kim, J. Y. Kang, P. E. Jeon, J. C. Chol, H. L. Park, and T. W. Kim, "GaN-Based white-light-emitting diodes fabricated with a mixture of $\text{Ba}_3\text{MgSi}_2\text{O}_8:\text{Eu}^{2+}$ and $\text{Sr}_2\text{SiO}_4:\text{Eu}^{2+}$ phosphors," *Jpn. J. Appl. Phys.*, vol. 43, no. 3, pp. 989–992, Mar. 2004.
- [4] J. K. Park, M. A. Lim, C. H. Kim, H. D. Park, J. T. Park, and S. Y. Choi, "White light-emitting diodes of GaN-based $\text{Sr}_2\text{SiO}_4:\text{Eu}$ and the luminescent properties," *Appl. Phys. Lett.*, vol. 82, pp. 683–685, Feb. 2003.
- [5] S. Muthu, F. J. P. Schuurmans, and M. D. Pashley, "Red, green, and blue LEDs for white light illumination," *IEEE J. Sel. Topics Quantum Electron.*, vol. 8, no. 2, pp. 683–685, Mar. 2003.
- [6] M. Yamada, Y. Narukawa, and T. Mukai, "Phosphor free high-luminous-efficiency white light-emitting diodes composed of InGaN multi-quantum well," *Jpn. J. Appl. Phys.*, vol. 41, no. 3A, pp. L246–L248, Mar. 2002.
- [7] A. Kikuchi, M. Kawai, M. Tada, and K. Kishino, "InGaN/GaN multiple quantum disk nanocolumn light-emitting diodes grown on (111) Si substrate," *Jpn. J. Appl. Phys.*, vol. 43, no. 12A, pp. L1524–L1526, Nov. 2004.
- [8] M. Achermann, M. A. Petruska, S. Kos, D. L. Smith, D. D. Koleske, and V. I. Klimov, "Energy-transfer pumping of semiconductor nanocrystals using an epitaxial quantumwell," *Nature*, vol. 429, pp. 642–646, Jun. 2004.
- [9] C. B. Murray, D. J. Norris, and M. G. Bawendi, "Synthesis and characterization of nearly monodisperse CdE ($E = \text{S}, \text{Se}, \text{Te}$) semiconductor nanocrystallites," *J. Amer. Chem. Soc.*, vol. 115, pp. 8706–8715, Mar. 1993.
- [10] A. P. Alivisatos, "Semiconductor clusters, nanocrystals, and quantum dots," *Science*, vol. 271, pp. 933–937, Feb. 1996.
- [11] B. O. Dabbousi, J. Rodriguez-Viejo, F. V. Mikulec, J. R. Heine, H. Mattoussi, R. Ober, K. F. Jensen, and M. G. Bawendi, "(CdSe)ZnS core-shell quantum dots: Synthesis and characterization of a size series of highly luminescent nanocrystallites," *J. Phys. Chem. B*, vol. 101, pp. 9463–9475, Jun. 1997.